Journal of Porous Materials (2023) 30:1011–1019
https://doi.org/10.1007/s10934-022-01394-z

The preparation of ultrathin and porous electrospinning membranes of HKUST-1/PLA with good antibacterial and filtration performances

Yanyan Zhu[1] · Dangsha Yang[1] · Jiangen Li[1] · Zhenqing Yue[1] · Jingheng Zhou[1] · Xinlong Wang[1]

Accepted: 18 November 2022 / Published online: 2 December 2022

Abstract
Developing degradable filter membranes that inhibit bacterial infection for preventing particle matter and infectious disease has been a research hotspot. Here, the fiber membranes of polylactic acid (PLA)/HKUST-1 with porous structure through the entire fiber matrix were prepared by electrospinning method. Due to the HKUST-1 incorporation and the presence of pore through fiber, the hydrophobicity of prepared membranes had been improved. The PLA/HKUST-1 membranes exhibited the good antibacterial activity against *Escherichia coli* and *Staphylococcus aureus*, and the antibacterial rate for *S. aureus* reached 99.99%. The filtration performance of PLA/HKUST-1 membranes was better than that of the melt-blown fabric although their thickness was only about one-third of the thickness of the currently commercial polypropylene melt-blown fabric.

Keywords MOFs · Antibacterial · Filtration · Electrospinning

1 Introduction

The effects of particulate matter (PM) with different sizes and highly infectious diseases such as COVID-19 on the human health have driven mankind to develop more effective protective materials [1–3]. Among them, the filter membrane is one of the most important materials, which can be widely used in various protective equipment such as protective face masks and antismog window screens. The electrospinning fiber membranes in filtration application have attracted considerable attention due to their small diameter, high surface-to-volume ratio, small inter-fiber pore sizes, low-cost and relatively high production rate [4–11], etc. By incorporating appropriate polymers with functional materials, degradable filter membranes can be prepared to solve the environmental problems caused by common non-degradable filter materials, and at the same time, the membranes can be endowed with functions such as antibacterial properties [12–14].

The morphology, hydrophilicity or hydrophobicity, filtration efficiency and pressure drop of the electrospinning composite membranes can be controlled by changing contents of particles added into the polymer matrix because the presence of particles could influence the roughness, chemistry, and porosity of the surface of the prepared membranes [15–17]. The incorporation of particles into electrospinning polymer nanofibers have been explored working in drug delivery [18, 19], water treatment, air filtration and antibacterial applications [14, 20–22]. A lot kind of particles such as SiO_2, Ag, TiO_2, and graphene oxides have been used for different purposes [23, 24]. Porous structures on the electrospinning fiber surface or through the entire fiber matrix can increase the surface to volume and broaden the range of applications for membranes. The preparation of porous polymer nanofibers with high surface areas is still a challenge.

Metal–organic frameworks (MOFs) are formed by the coordination of metal ions with organic ligands, and have the advantages of high specific surface area, large porosity, variable structure, and adjustable channel [24–26]. MOFs have become the attractive antimicrobial materials for applications in which a tunable antibacterial agent is required. Different from the action mechanism of small molecular antibacterial agents, the antibacterial performance of MOFs is mainly due to release of metal ions (such as Ag^+, Cu^{2+}, Zn^{2+}, and Co^{2+}) from structure collapse, which destroy the cell membrane, lipid peroxidation, and DNA degradation to kill bacteria [27–30].

In this study, the fiber membranes with a porous structure consisted of polylactic acid (PLA) and HKUST-1 were prepared by electrospinning method. PLA was a biodegradable

✉ Xinlong Wang
wxinlong323@163.com

[1] School of Chemical Engineering, Nanjing University of Science & Technology, Nanjing 210094, China

polymer [31], which could be degraded into CO_2 and H_2O. As a kind of Cu-MOFs, HKUST-1 had previously been reported to have good antibacterial activity against *Candida albicans*, *Aspergillus niger* and *Aspergillus oryzae* etc. [1, 12]. Therefore, the prepared membranes had biodegradability and antibacterial performance. When they were used as filter material, they could overcome the environmental problems caused by the non-degradable polypropylene melt blown cloth which was widely used as at present. In addition, due to its good antibacterial performance, the membranes could reduce the influence of bacteria and other microorganisms in the air on people's health.

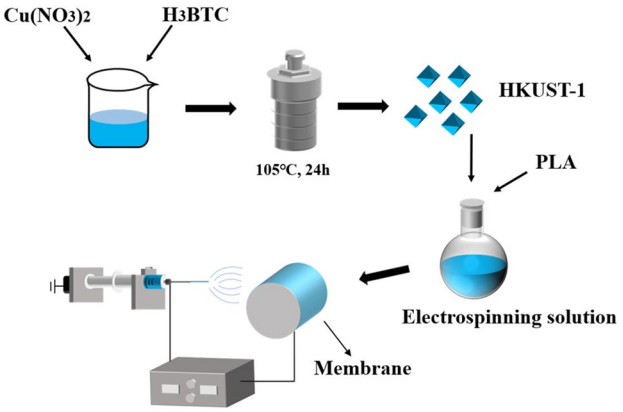

Fig. 1 The preparation process of membranes

2 Experimental

2.1 The preparation of HKUST-1

HKUST-1 was synthesized by the hydrothermal method [30]. $Cu(NO_3)_2{\cdot}3H_2O$ (12 mM) was dissolved in 25 mL of deionized water and 8 mM of H_3BTC was dissolved in 25 mL of DMF. At room temperature, the two solutions were mixed and stirred for 10 min. The mixture was transferred into the reaction kettle and kept in the oven at 105 ℃ for 24 h. The HKUST-1 particles were obtained by centrifugation and washed with water and ethanol for three times, respectively.

2.2 Preparation of the fiber membranes

PLA (18 g) and 105.6 g of dichloromethane (DCM) were added to a round-bottomed flask, and the mixture was sealed and stirred for 2 h to dissolve PLA in DCM completely. The HKUST-1 particles in DMF suspension were put it into the above round-bottomed flask and stirred to obtain electrospinning solution (The HKUST-1 content was 0, 0.6, and 3.0 wt% of the PLA mass and the ratio of DCM to DMF was 8:2). Then, the spinning solution was pit into a syringe. The electrospinning process proceeded under 18 kV. The receiving distance was set as 17 cm and the pushing injection speed was 0.004 mm/s. The temperature and the humidity were controlled at about 40 ℃ and 50–80% respectively. The fiber membranes with a thickness of about 0.036 mm were obtained and named as PLA, PLA-K0.6 and PLA-K3 according to the content of HKUST-1 (0, 0.6, and 3.0 wt%) in sequence. Figure 1 showed the preparation process of membranes.

2.3 General characterization

Field emission scanning electron microscope (FEI Quanta 250FEG) was used to observe the surface morphology of the samples. X-ray Diffraction (XRD, Bruker D8-ADVANCE) was performed on Cu Kα radiation with a range of 5°–70°. The Fourier transform infrared test was performed with Shimadzu 8400S and the scanning range was 400–4000 cm^{-1}. TGA was carried on the GA/SDTA85 (DTG, Shimadzu DTG-60) between 20 and 800 ℃ in a nitrogen atmosphere. The concentration of Cu^{2+} released from PLA-K3 was obtained by inductively coupled plasma mass spectrometry (ICP-MS, ThermoFisher I CAPQ). The membrane was cut discs with a diameter of 5 cm and immersed in water. The bottle with water and discs was placed in a constant temperature oscillator to shake for different time. Then, the solution was centrifuged for detection. The tensile test of the membrane was carried out with the TY8000A-500N electromechanical universal testing machine (Jiangsu Tianyuan Testing Equipment Co., Ltd) in accordance with the ASTMD638 standard. The sample was 4 cm × 0.5 cm. The speed was 10 N/min and each sample was tested for 5 times.

2.4 Antibacterial test of fiber membrane

The antibacterial abilities of fiber membranes were evaluated by bacterial colony counting method using *Escherichia coli* and *Staphylococcus aureus* [7]. The target bacteria were cultivated at 37 ℃ in Luria–Bertani broth until the bacteria concentration was at approximately 10^9 CFU/mL. The concentration of bacterial suspension was diluted with sterile water to (1–5) × 10^6 CFU/mL. Then, 2 mL of 10^6 CFU/mL suspension was put into 40 mL water suspension containing the membrane discs of 5 cm diameter. The bottles with mixture were set on the shaker at 37 ℃ and shaken for 24 h. Subsequently, 1 mL of suspension after shake period was cultivated at 37 ℃. The antibacterial rate (R) was calculated via the Eq. (1):

$$R(\%) = \frac{N_0 - N}{N_0} * 100 \quad (1)$$

where N_0 and N are the average number of viable bacteria on a reference sample without discs and on the sample containing discs after antibacterial tests, respectively. Each sample was tested for 3 times.

2.5 PM filtration measurement

The PM adsorption experiment was carried out with a self-assembled experimental device as shown in Fig. S1 [4, 16, 20]. The dust detector was the LD-5/J laser dust meter from Nanjing Trinyaer Environmental Protection Technology Co., Ltd. The PM particles were produced by burning cigarette in the upper container. The prepared membrane was cut into 7 cm × 7 cm square and sandwiched between upper and lower containers. The air in the upper container was drawn through the prepared membrane into the lower container using a vacuum pump at a flow rate of 2 L/min. The removal efficiency *Re* was calculated via Eq. (2):

$$\mathrm{Re} = \frac{\mathrm{C_{above}} - \mathrm{C_{below}}}{\mathrm{C_{above}}} \times 100\% \quad (2)$$

where C_{above} was the PM concentration in the upper container (μg/m^3) and C_{below} was the PM concentration in the lower container (μg/m^3).

2.6 Statistical analysis

One-way analysis of variance (ANOVA) with Tukey's post hoc test was used for statistical analysis of between-group and within-group data. The *$p < 0.05$, **$p < 0.01$ and ***$p < 0.001$ were accepted as statistically significant.

3 Results and discussion

3.1 The morphology of fiber membranes

The HKUST-1 particles were synthesized through the solvothermal reaction according to the previous report. The SEM image, XRD and IR of the prepared HKUST-1 were displayed in Fig. S2. The HKUST-1 particles had the octahedral morphology and their size was about 16 μm. The results of XRD and IR were consistent with the literature as reported [30]. Figure 2 showed the morphology of the fiber membranes. The fibers with diameter of about 1 μm were stacked together and many interspaces were formed. As seen from the enlarged image in the upper right corner, every fiber contained a large number of nano pores which were through the entire fiber. The formation of pores on the fiber primarily was attributed to the phase separation of the different components of the electrospinning solution, specifically, the separation between the polymers and solvents, the separation between the polymers and the non-solvents [32, 33]. The existence of pores on fiber was beneficial to increase the surface to volume or surface to weight ratio of the fiber membranes. Because the size of HKUST-1 particles was larger than the diameter of fibers, it could be seen that they were wrapped on the membrane by the intersecting fibers. The mapping of Cu showed that the HKUST-1 particles were dispersed uniformly in the membrane containing 0.6 wt% of HKUST-1. However, the agglomeration of HKUST-1 particles could be observed for PLA-K3 containing 3 wt% of HKUST-1 [4].

3.2 The contact angles and mechanical properties of fiber membranes

The contact angle was related to the surface roughness and chemical properties of the material, which could reflect the wettability of the fiber membrane and directly affected the adsorption of bacteria or pollution particles on the surface [34, 35]. As shown in Fig. 3a, the contact angle of the PLA membrane was 72.31°, and the values for PLA-K0.6 and PLA-K3 were increased 83.41° and 92.54°, respectively. Both the embedded HKUST-1 particles on membrane surface and the resulting change in the chemical composition in the surface increased the contact angle. As shown in Fig. 3b, the tensile strength of PLA membrane was 1.43 MPa. When 0.6 wt% of HKUST-1 was added, the tensile strength of PLA-K0.6 membrane was 2.28 MPa. However, the tensile strength of PLA-K3 membrane was slightly reduced to 2.00 MPa. It was reported that the MOF particles in the composites could effectively transfer stresses and lead to the enhancement in tensile strength [36, 37]. As the amount of MOF increased, agglomeration of particles occurred, which weakened the inter-fiber forces and reduced the tensile strength [7]. (A typical stress–strain curve was shown in Fig. S3).

3.3 Antibacterial rate of HKUST-1/PLA fiber membranes

The antibacterial properties of prepared fiber membranes against both Gram-positive *Staphylococcus aureus* and Gram-negative *E. coli* were assessed and shown in Fig. 4. The neat PLA membrane adsorbed bacteria as had frequently been proved [36]. When *E. coli* contacting with PLA-K3, the number of colonies in the petri dishes was reduced compared with PLA membrane and the antibacterial rate was 91%. For *S. aureus*, there were no colonies growing in the petri dishes (Fig. 4) and the antibacterial rate reached 99.99%

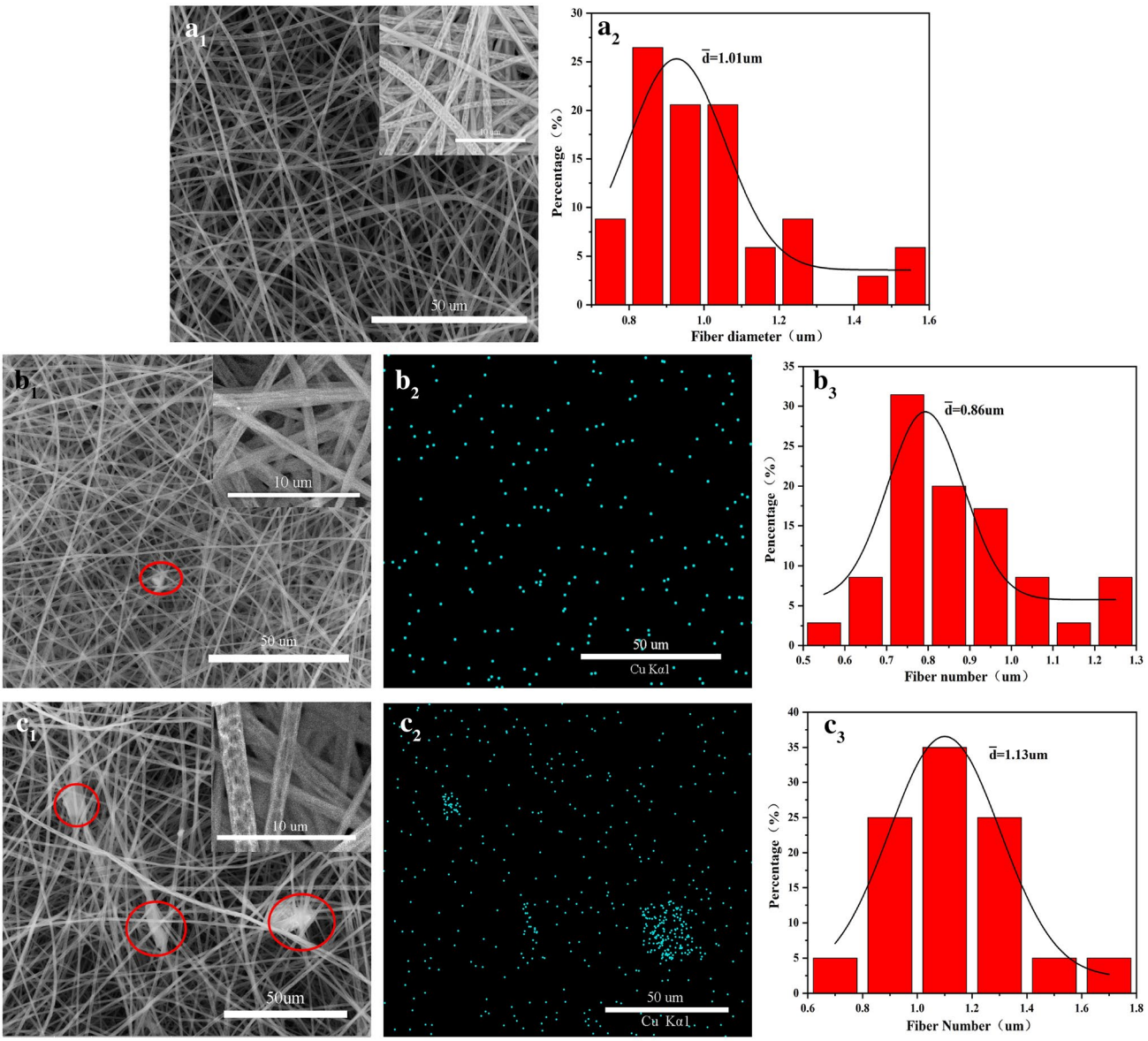

Fig. 2 The SEM of **a** PLA; **b** PLA-K0.6; **c** PLA-K3

(Fig. 5a) with PLA-K3. The enhancement in bactericidal properties for fiber membranes with HKUST-1 was mainly due to release of Cu^{2+} from HKUST-1 in the membrane. Figure 5b showed the Cu^{2+} concentration change in solution when PLA-K3 was soaked in water at different time. The concentration of Cu^{2+} in solution gradually increased and reached a maximum of 22.06 ppb at 12 h. Then, the concentration of Cu^{2+} in the solution began to decrease. The Cu^{2+} from the release of PLA-K3 entered the bacterial cell, and damaged the structure of DNA and some essential enzymes [24, 38–40].

The bacterial morphologies cultured on PLA membrane and PLA-K3 were compared in Fig. 6 to further understand the antibacterial mechanism of the membranes. On the PLA membrane, *E. coli* and *S. aureus* exhibited smooth surface and intact morphology with rod and rounded shapes, respectively. However, they clumped, deformed, collapsed, and even dissolved on the PLA-K3 membrane. Table 1 showed the comparison of the antibacterial rates of the prepared membranes against *E. coli* and *S. aureus* with those reported. The presence of pores on the fibers increased the specific

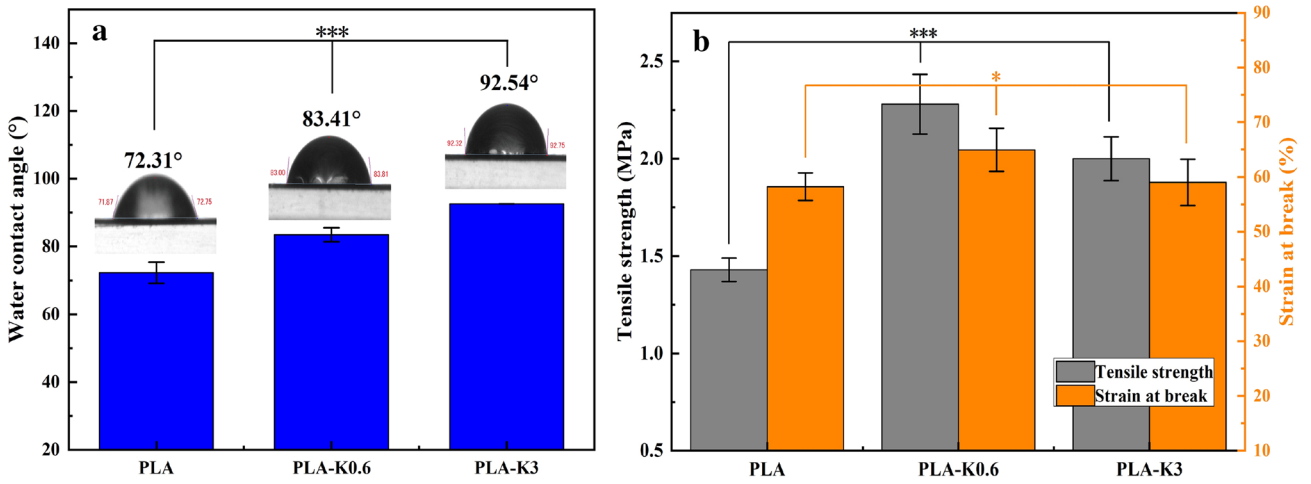

Fig. 3 Bar diagram of contact angle (**a**) and mechanical properties (**b**) of fiber membranes

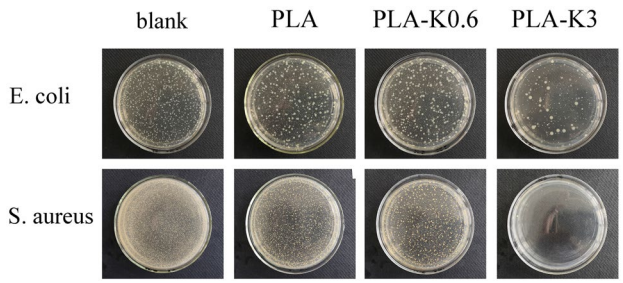

Fig. 4 Agar plate experiment of antibacterial activity of PLA and PLA-K **a** *E. coli*; **b** *S. aureus*

surface area of the membrane, which would help bacteria to adhere on the surface of membrane and Cu^{2+} to find bacteria quickly after release. Therefore, the membrane had a good antibacterial effect when the addition amount of HKUST-1 was only 3 wt%.

3.4 Filtration performance of HKUST-1/PLA fiber membranes

The photos of the filtration effect to PM2.5 and PM10 of the HKUST-1/PLA fiber membranes at different time were shown in Fig. S4. It could be seen that the membrane had good filtration performance in the case

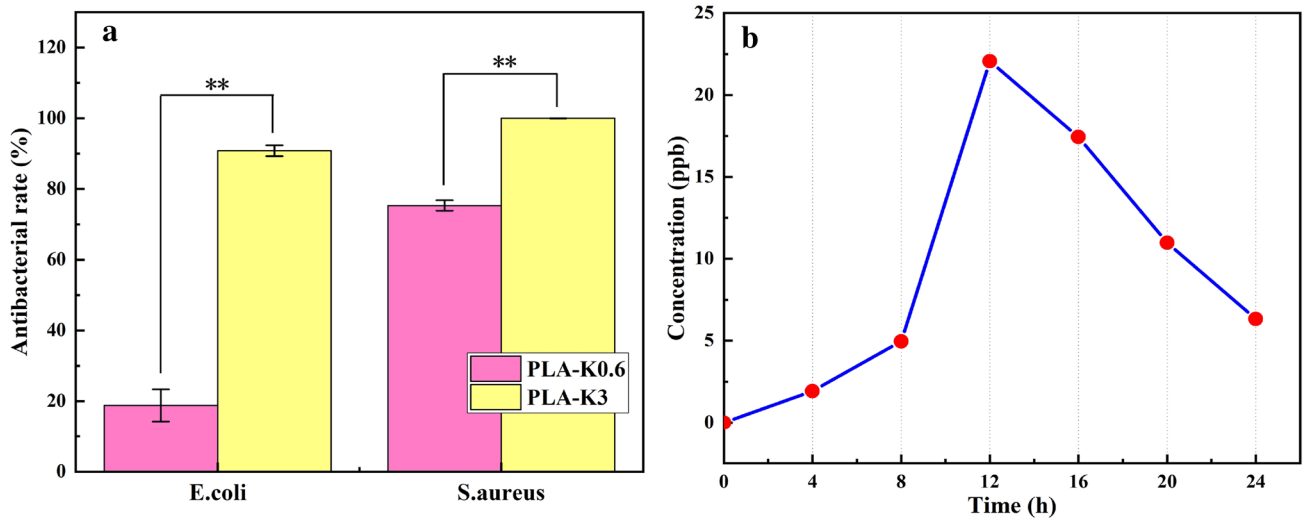

Fig. 5 **a** Antibacterial rate of *E. coli* and *S. aureus* by PLA-K; **b** Cu^{2+} release curves of PLA-K3 in aqueous solution at different time

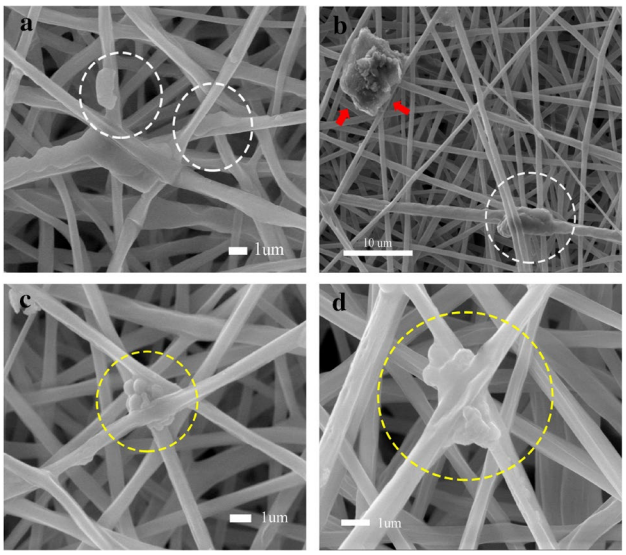

Fig. 6 SEM images of PLA (**a**) and PLA-K3 (**b**) after 24 h in *E. coli*; SEM images of PLA (**c**) and PLA-K3 (**d**) after 24 h in *S. aureus*

Table 1 Comparison of antibacterial rate of HKUST-1/PLA membrane with others

Fiber membranes	Antibacterial rate (%)		References
	E	S	
PLA-K3	91	99.99	This work
1.7%$CuCl_2L_2$/CA	75	80	[41]
9.1%Cu-MOFs/PLA	99	99	[42]
10%HKUST-1/CS/PVA	99	99	[39]
GO/SF	64	58	[43]

of high concentration or low concentration of PM. Figure 7a showed the filtration efficiency curves of melt-blown fabric (MB) and PLA-K3 with time. It was obvious that the filtration performance of PLA-K3 was very stable. The filtration efficiency of PLA-K3 for PM2.5 and PM10 was close to 100% within filtration time, while the filtration efficiency of MB fabric was only 24% at 2 min. Then, the filtration efficiency slowly increased with time but it was still lower than that of the PLA-K3. The above results showed that the filtration efficiency of the prepared fiber membrane was higher than that of the melt-blown fabric, especially in the high concentration PM2.5 environment, where the filtration efficiency was four times higher than that of the melt-blown fabric. In addition, PLA-K3 had the advantage of being ultra-thin with a thickness of 0.036 mm, which was only 1/3 of that of melt-blown cloth. This would reduce the amount of polymer used, thereby lightening the environmental burden that may be caused by the large-scale application of non-degradable polymers. However, it can be seen in Fig. 7b that the PLA-K3 had higher pressure drop than that of the melt-blown fabric. Table 2 showed a comparison of the filtration efficiency for PM2.5 between PLA-K3 membrane and other spinning membranes reported. The quality factor of PLA-K3 was 0.063, which was sufficient to demonstrate its good filtration performance further. SEM was used to observe the membrane after filtration as shown in Fig. 7e and f, and a lot of deposits were observed on the membranes.

4 Conclusion

HKUST-1 particles were prepared and incorporated into the PLA electrospinning fiber membranes. When the HKUST-1 content was 3.0 wt%, the removal efficiency was clos to 100% for PM2.5 and PM10 within 20 min and the quality factor of PLA-K3 was 0.063. The PLA-K3 had an antibacterial rate of 99.99% for *S. aureus*. The prepared membrane could be used in the field of masks instead of melt-blown fabric of polypropylene, and solved the problem of non-degradability and non-functionalization of melt-blown fabric.

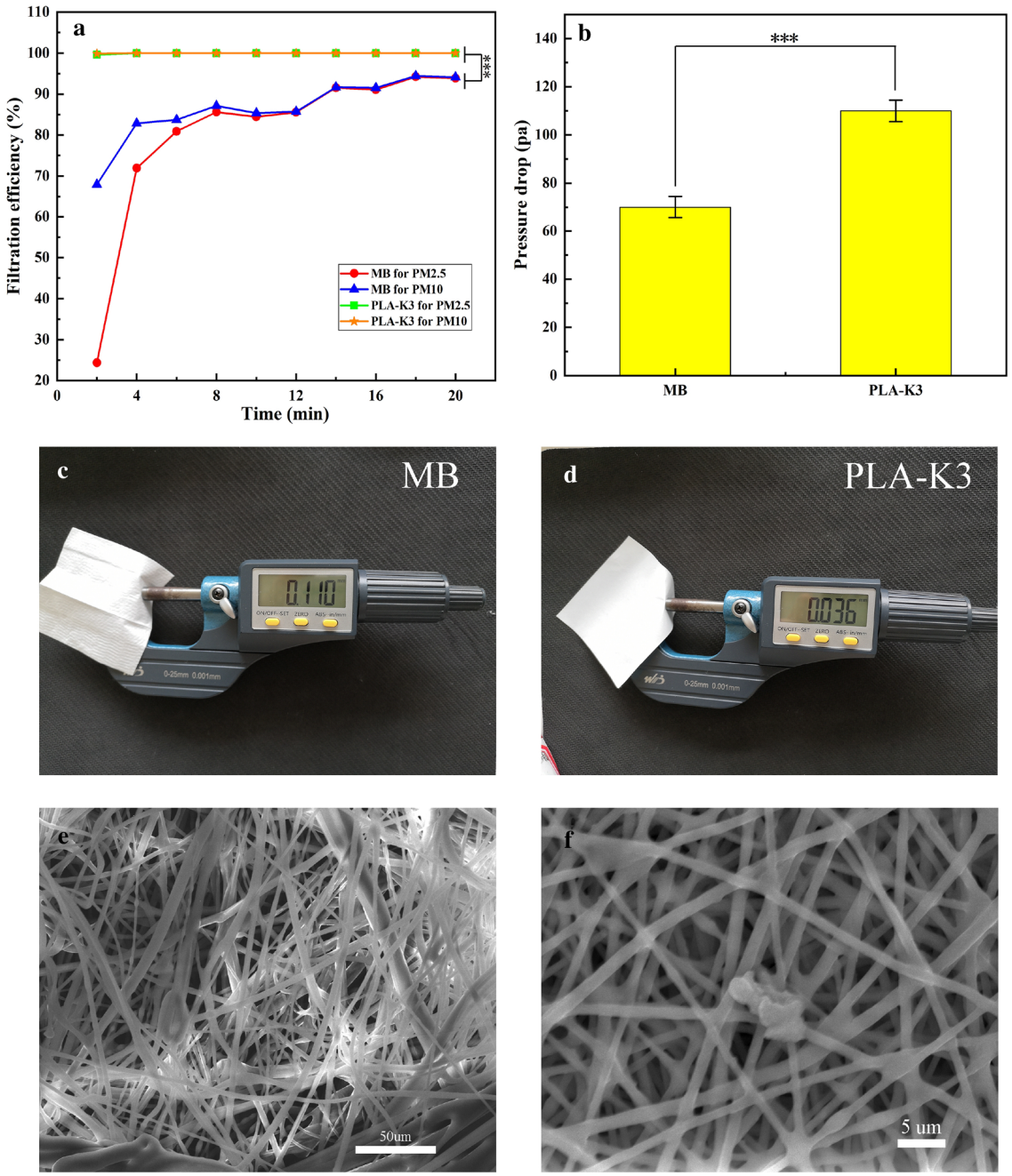

Fig. 7 The filtering efficiency of MB and PLA-K3 at different time (**a**); the pressure drop of MB and PLA-K3 (**b**); thickness of melt-blown fabric (**c**) and PLA-K3 (**d**); SEM of the membranes after adsorption (**e**) MB and (**f**) PLA-K3

Table 2 Comparison of particle filtration efficiency of PLA-K3 with others

Fiber membranes	Particle (um)	η (%)	ΔP (Pa)	Q_f	References
MB	2.5	80.4	70	0.023	This work
3%HKUST-1/PLA	2.5	99.9	110	0.063	This work
9%ZIF-8/9%PAA	5	99.6	172	0.03	[4]
2.5%ZIF-8/PP/PVA	0.2–4.6	96.5	34	0.099	[17]
GO/PI-6/PAN	2.5	99.5	92	0.058	[20]

Supplementary Information The online version contains supplementary material available at https://doi.org/10.1007/s10934-022-01394-z.

Acknowledgements This work was supported by Science and Technology Support Program (Social Development) of Jiangsu Province of China (BE 2020709) and Priority Academic Program Development of Jiangsu Higher Education Institutions (PAPD).

Author contributions All authors contributed to the study conception and design. The manuscript was written by YZ and revised by XW. Material preparation, data collection and analysis were performed by DY and JL. The data verification was done by ZY and JZ. All authors commented on previous versions of the manuscript. Final manuscript read and approved by all authors.

Declarations

Conflict of interest The authors declared that they have no conflicts of interest to this work.

References

1. N.A. Khan, Z. Hasan, S.H. Jhung, Adsorptive removal of hazardous materials using metal-organic frameworks (MOFs): a review. J. Hazard. Mater. **244–245**, 444–456 (2013). https://doi.org/10.1016/j.jhazmat.2012.11.011
2. A. Tomczak, A.B. Miller, S.A. Weichenthal, Long-term exposure to fine particulate matter air pollution and the risk of lung cancer among participants of the Canadian National Breast Screening Study. Int. J. Cancer **139**, 1958–1966 (2016). https://doi.org/10.1002/ijc.30255
3. L.S.E. Jack, C.S. Ulrik, Physical activity, air pollution, and the risk of asthma and chronic obstructive pulmonary disease. Am. J. Respir. Crit. Care Med. **194**, 855–865 (2016). https://doi.org/10.1164/rccm.201510-2036OC
4. J. Guo, A. Hanif, J. Shang, PAA@ZIF-8 incorporated nanofibrous membrane for high-efficiency PM2.5 capture. Chem. Eng. J. **405**, 126584 (2021). https://doi.org/10.1016/j.cej.2020.126584
5. H. Chen, A. Malheiro, C. Blitterswijk, Direct writing electrospinning of scaffolds with multidimensional fiber architecture for hierarchical tissue engineering. ACS Appl. Mater. Interfaces **9**, 38187–38200 (2017). https://doi.org/10.1021/acsami.7b07151
6. M. Zhu, J. Li, J. Yu, Superstable and intrinsically self-healing fibrous membrane with bionic confined protective structure for breathable electronic skin. Angew. Chem. Int. Ed. Engl. **61**, e202200226 (2022). https://doi.org/10.1002/anie.202200226
7. X. Zheng, Y. Zhang, L. Zou, Robust ZIF-8/alginate fibers for the durable and highly effective antibacterial textiles. Colloid Surf. B **193**, 111127 (2020). https://doi.org/10.1016/j.colsurfb.2020.111127
8. J. Yin, L. Xu, Batch preparation of electrospun polycaprolactone/chitosan/aloe vera blended nanofiber membranes for novel wound dressing. Int. J. Biol. Macromol. **160**, 352–363 (2020). https://doi.org/10.1016/j.ijbiomac.2020.05.211
9. C. Cleeton, A. Keirouz, X. Chen, Electrospun nanofibers for drug delivery and biosensing. ACS Biomater. Sci. Eng. **5**, 4183–4205 (2019). https://doi.org/10.1021/acsbiomaterials.9b00853
10. W. Li, T. Luo, Y. Yang, Formation of controllable hydrophilic/hydrophobic drug delivery systems by electrospinning of vesicles. Langmuir **31**, 5141–5146 (2015). https://doi.org/10.1021/la504796v
11. Y. Xu, J.-W. Zhu, J.-B. Fang, Electrospun high-thermal-resistant inorganic composite nonwoven as lithium-ion battery separator. J. Nanomater. **2020**, 1–10 (2020). https://doi.org/10.1155/2020/3879040
12. J.E. Cun, X. Fan, Q.Q. Pan, Copper-based metal-organic frameworks for biomedical applications. Adv. Colloid Interface **305**, 102689 (2022). https://doi.org/10.1016/j.cis.2022.102686
13. C. Fleuret, A.S. Andreani, E. Laine, Complex wing spar design in carbon fiber reinforced composite for a light aerobatic aircraft. Mech. Ind. **17**, 19 (2016). https://doi.org/10.1051/meca/2016032
14. T. Lu, J. Cui, Q. Qu, Multistructured electrospun nanofibers for air filtration: a review. ACS Appl. Mater. Interfaces **13**, 23293–23313 (2021). https://doi.org/10.1021/acsami.1c06520
15 Y. Deng, T. Lu, J. Cui, Morphology engineering processed nanofibrous membranes with secondary structure for high-performance air filtration. Sep. Purif. Technol. **294**, 121093 (2022). https://doi.org/10.1016/j.seppur.2022.121093
16. Q.-H. Zhu, G.-H. Zhang, L. Zhang, Self-charge-carrying air filter by in situ polymerization to avoid charge dissipation and potential material poisoning. Chem. Eng. J. **449**, 13778 (2022). https://doi.org/10.1016/j.cej.2022.137788
17 T.T. Li, Y. Fan, X. Cen, Polypropylene/polyvinyl alcohol/metal-organic framework-based melt-blown electrospun composite membranes for highly efficient filtration of PM2.5. Nanomaterials **10**, 2025 (2020). https://doi.org/10.3390/nano10102025
18. S. Gautam, J. Singhal, H.K. Lee, Drug delivery of paracetamol by metal-organic frameworks (HKUST-1): improvised synthesis and investigations. Mater. Today Chem. **23**, 100647 (2022). https://doi.org/10.1016/j.mtchem.2021.100647
19. P. Horcajada, T. Chalati, C. Serre, Porous metal-organic-framework nanoscale carriers as a potential platform for drug delivery and imaging. Nat. Mater. **9**, 172–178 (2010). https://doi.org/10.1038/nmat2608
20 H. Dai, X. Liu, C. Zhang, Electrospinning polyacrylonitrile/graphene oxide/polyimide nanofibrous membranes for High-efficiency PM2.5 filtration. Sep. Purif. Technol. **276**, 119243 (2021). https://doi.org/10.1016/j.seppur.2021.119243
21. Y. Xiao, Y. Wang, W. Zhu, Development of tree-like nanofibrous air filter with durable antibacterial property. Sep. Purif. Technol. **259**, 118135 (2021). https://doi.org/10.1016/j.seppur.2020.118135
22. C. Zhang, L. Yao, Z. Yang, Graphene oxide-modified polyacrylonitrile nanofibrous membranes for efficient air filtration. ACS Appl. Nano Mater. **2**, 3916–3924 (2019). https://doi.org/10.1021/acsanm.9b00806
23. Z. Rahmati, J. Abdi, M. Vossoughi, Ag-doped magnetic metal organic framework as a novel nanostructured material for highly efficient antibacterial activity. Environ. Res. **188**, 109555 (2020). https://doi.org/10.1016/j.envres.2020.109555
24. Y.N. Slavin, J. Asnis, U.O. Hafeli, Metal nanoparticles: understanding the mechanisms behind antibacterial activity. J. Nanobiotechnol. **15**, 65 (2017). https://doi.org/10.1186/s12951-017-0308-z
25. N. Zhu, Y. Zou, M. Huang, A sensitive, colorimetric immunosensor based on Cu-MOFs and HRP for detection of dibutyl phthalate

in environmental and food samples. Talanta **186**, 104–109 (2018). https://doi.org/10.1016/j.talanta.2018.04.023
26. R. Adam, M. Mon, R. Greco, Self-assembly of catalytically active supramolecular coordination compounds within metal-organic frameworks. J. Am. Chem. Soc. **141**, 10350–10360 (2019). https://doi.org/10.1021/jacs.9b03914
27 M.D. Firouzjaei, A.A. Shamsabadi, M. Sharifian Gh, A novel nanocomposite with superior antibacterial activity: a silver-based metal organic framework embellished with graphene oxide. Adv. Mater. Interfaces **5**, 1701365 (2018). https://doi.org/10.1002/admi.201701365
28. M.N. Hasan, A. Bera, T.K. Maji, Sensitization of nontoxic MOF for their potential drug delivery application against microbial infection. Inorg. Chim. Acta **523**, 120381 (2021). https://doi.org/10.1016/j.ica.2021.120381
29. H. Wang, D. Yu, J. Fang, Renal-clearable prphyrinic metal-organic framework nanodots for enhanced photodynamic therapy. ACS Nano **13**, 9206–9217 (2019). https://doi.org/10.1021/acsnano.9b03531
30. S. Bouson, A. Krittayavathananon, N. Phattharasupakun, Antifungal activity of water-stable copper-containing metal-organic frameworks. R. Soc. Open Sci. **4**, 170654 (2017). https://doi.org/10.1098/rsos.170654
31 Y. Deng, T. Lu, J. Cui, Bio-based electrospun nanofiber as building blocks for a novel eco-friendly air filtration membrane: a review. Sep. Purif. Technol. **277**, 119623 (2021). https://doi.org/10.1016/j.seppur.2021.119623
32. P.Y. Chen, S.H. Tung, One-step electrospinning to produce non-solvent-induced macroporous fibers with ultrahigh oil adsorption capability. Macromolecules **50**, 2528–2534 (2017). https://doi.org/10.1021/acs.macromol.6b02696
33. C.L. Li, D.M. Wang, A. Deratani, Insight into the preparation of poly(vinylidene fluoride) membranes by vapor-induced phase separation. J. Membr. Sci. **361**, 154–166 (2010). https://doi.org/10.1016/j.memsci.2010.05.064
34. Y. Liu, D. Wang, Z. Sun, Preparation and characterization of gelatin/chitosan/3-phenylacetic acid food-packaging nanofiber antibacterial films by electrospinning. Int. J. Biol. Macromol. **169**, 161–170 (2021). https://doi.org/10.1016/j.ijbiomac.2020.12.046
35. L. Deng, X. Zhang, Y. Li, Characterization of gelatin/zein nanofibers by hybrid electrospinning. Food Hydrocolloid **75**, 72–80 (2018). https://doi.org/10.1016/j.foodhyd.2017.09.011
36. S.Z.H. Kiadeh, A. Ghaee, M. Farokhi, Electrospun pectin/modified copper-based metal-organic framework (MOF) nanofibers as a drug delivery system. Int. J. Biol. Macromol. **173**, 351–365 (2021). https://doi.org/10.1016/j.ijbiomac.2021.01.058
37. A. Ghaee, M. Karimi, M. Lotfi-Sarvestani, Preparation of hydrophilic polycaprolactone/modified ZIF-8 nanofibers as a wound dressing using hydrophilic surface modifying macromolecules. Mater. Sci. Eng. C **103**, 109767 (2019). https://doi.org/10.1016/j.msec.2019.109767
38. S. Shams, W. Ahmad, A.H. Memon, Cu/H_3BTC MOF as a potential antibacterial therapeutic agent against *Staphylococcus aureus* and *Escherichia coli*. New J. Chem. **44**, 17671–17678 (2020). https://doi.org/10.1039/d0nj04120c
39. S. Wang, F. Yan, P. Ren, Incorporation of metal-organic frameworks into electrospun chitosan/poly (vinyl alcohol) nanofibrous membrane with enhanced antibacterial activity for wound dressing application. Int. J. Biol. Macromol. **158**, 9–17 (2020). https://doi.org/10.1016/j.ijbiomac.2020.04.116
40. C. Pettinari, R. Pettinari, C. Di Nicola, Antimicrobial MOFs. Coord. Chem. Rev. **446**, 214121 (2021). https://doi.org/10.1016/j.ccr.2021.214121
41. R.E. Demirdogen, D. Kilic, F.M. Emen, Novel antibacterial cellulose acetate fibers modified with 2-fluoropyridine complexes. J. Mol. Struc. **1204**, 127537 (2020). https://doi.org/10.1016/j.molstruc.2019.127537
42. Z. Liu, J. Ye, A. Rauf, A flexible fibrous membrane based on copper(II) metal-organic framework/poly(lactic acid) composites with superior antibacterial performance. Biomater. Sci. **9**, 3851–3859 (2021). https://doi.org/10.1039/d1bm00164g
43. S.D. Wang, Q. Ma, K. Wang, Improving Antibacterial activity and biocompatibility of bioinspired electrospinning silk fibroin nanofibers modified by graphene oxide. ACS Omega **3**, 406–413 (2018). https://doi.org/10.1021/acsomega.7b01210